Cell Cycle Heritability and Localization Phase Transition in Growing Populations

Takashi Nozoe[1] and Edo Kussell[1,2]
[1]Department of Biology, New York University, 12 Waverly Place, New York, New York 10003, USA
[2]Department of Physics, New York University, 726 Broadway, New York, New York 10003, USA

(Received 7 April 2020; accepted 27 October 2020; published 29 December 2020)

The cell cycle duration is a variable cellular phenotype that underlies long-term population growth and age structures. By analyzing the stationary solutions of a branching process with heritable cell division times, we demonstrate the existence of a phase transition, which can be continuous or first order, by which a nonzero fraction of the population becomes localized at a minimal division time. Just below the transition, we demonstrate the coexistence of localized and delocalized age-structure phases and the power law decay of correlation functions. Above it, we observe the self-synchronization of cell cycles, collective divisions, and the slow "aging" of population growth rates.

DOI: 10.1103/PhysRevLett.125.268103

The duration of a cell cycle, or the interdivision time (IDT), is a fluctuating quantity in cellular populations, and its statistical properties are thought to result from biological mechanisms that regulate cell growth and division [1–5]. In most observations on mammalian cells and in a subset of bacterial experiments, positive mother-daughter correlations of IDTs have been measured (see Table S1 in [6]). In general, the heritability of a trait (i.e., a positive parent-offspring correlation) enables selection to act on the trait distribution in a population to increase the long-term population growth rate. In this Letter, we take up the question of how selection and cell cycle heritability interact to determine long-term population dynamics, a fundamental step toward understanding how evolution has shaped cell cycle control mechanisms. Our work makes connections between the dynamics of age-structured populations [32] and the error-threshold phenomena of evolutionary theory [7,33] and is applicable in experimental analyses of cellular population dynamics.

Model and stationary solutions.—We model a proliferating population by a branching process in which $K(\tau,\tau')$ is the transition probability density from τ' to τ, where τ' and τ are the parent and offspring IDTs, respectively. We focus on the analytically tractable Lebowitz-Rubinow model [34], which uses the transition kernel

$$K(\tau,\tau') = h\delta(\tau-\tau') + (1-h)k(\tau), \tag{1}$$

where $\delta(\cdot)$ is the Dirac delta function showing accurate inheritance of the parent's IDT, h represents the heritability of IDTs in the model ($0 \le h < 1$), and $k(\tau)$ is a probability density function on the interval (τ_0,∞), with $0 < \tau_0 < \infty$. A cell produces $\hat{z}$ offspring at every division, where $\hat{z}$ is independently drawn from a fixed probability distribution and its average is denoted by $z > 0$. The dynamics of cell divisions in the population are governed by

$$n_{\mathrm{div}}(\tau; t+\tau) = z\int_0^\infty K(\tau,\tau')n_{\mathrm{div}}(\tau';t)d\tau', \tag{2}$$

where $n_{\mathrm{div}}(\tau;t)d\tau dt$ is the expected number of dividing cells (cells at the termination of a cell cycle) between times t and $t+dt$ with IDT between τ and $\tau+d\tau$ [35]. The expected number of divisions occurring between t and $t+dt$ is given by $N_{\mathrm{div}}(t)dt := dt\int_0^\infty n_{\mathrm{div}}(\tau;t)d\tau$, and the time-dependent population growth rate is defined by $\Lambda_t := (z-1)N_{\mathrm{div}}(t)/N(t)$, where $N(t)$ is the expected population size at time t (see [6] for detailed derivations).

The steady-state, exponentially growing solution of Eq. (2) is characterized by the time-independent growth rate Λ and the probability density $p_{\mathrm{div}}(\tau)$ of IDTs of dividing cells, which can be found by substituting the form $n_{\mathrm{div}}(\tau;t) = N_{\mathrm{div}}(t)p_{\mathrm{div}}(\tau)$, where $N_{\mathrm{div}}(t)$ is proportional to $e^{\Lambda t}$, yielding

$$p_{\mathrm{div}}(\tau) = ze^{-\Lambda\tau}\int_0^\infty K(\tau,\tau')p_{\mathrm{div}}(\tau')d\tau'. \tag{3}$$

Using Eq. (1) and solving the above equation, one obtains

$$p_{\mathrm{div}}(\tau) = q_{h,\Lambda}(\tau) \tag{4}$$

where

$$q_{h,\Lambda}(\tau) := \frac{(1-h)k(\tau)ze^{-\Lambda\tau}}{1-hze^{-\Lambda\tau}}, \tag{5}$$

which is a valid solution if there exists Λ such that $q_{h,\Lambda}(\tau) \ge 0$ for all $\tau \in (\tau_0,\infty)$, and which normalizes $p_{\mathrm{div}}(\tau)$, i.e., Λ is the unique real solution of $Q(h,\Lambda) = 1$, where

$$Q(h,\Lambda) \coloneqq \int_0^\infty q_{h,\Lambda}(\tau)d\tau. \tag{6}$$

If $z=1$, for example, then $\Lambda=0$ and $p_{\rm div}(\tau)=k(\tau)$ for any $0\le h<1$; this can be realized as an isolated single cell, where offspring at each division event are removed.

In the absence of IDT heritability ($h=0$), one recovers the well-known result $p_{\rm div}(\tau)=ze^{-\Lambda\tau}k(\tau)$ where Λ is the unique real root of the integral equation $z\int_0^\infty e^{-\Lambda\tau}k(\tau)d\tau=1$ [3,36]. For $h>0$, one additionally must have $1-hze^{-\Lambda\tau}>0$ for all τ in the support of $k(\tau)$ to ensure $q_{h,\Lambda}(\tau)\ge 0$. If $k(\tau)>0$ for all $\tau>\tau_0$, we find

$$\Lambda \ge \omega_0(h) \coloneqq \sup_{\tau>\tau_0}\frac{\ln(hz)}{\tau} = \max\left[0,\frac{\ln(hz)}{\tau_0}\right] \tag{7}$$

[see [6] for $k(\tau)$ with bounded support]. Since $Q(h,\Lambda)$ is a monotonically decreasing function of Λ tending to zero as $\Lambda\to\infty$, $Q(h,\Lambda)=1$ has a unique root $\Lambda=\Lambda(h)$ provided that $Q(h,\omega_0(h))\ge 1$. This condition holds for $h<h_c$, where h_c is a heritability threshold defined by

$$Q(h_c,\omega_0(h_c))=1 \tag{8}$$

such that for $h>h_c$, $Q(h,\omega_0(h))<1$ and $Q(h,\Lambda)=1$ does not admit a real root Λ. For $h>h_c$, the solution $p_{\rm div}(\tau)$ given in Eq. (4) is incomplete as there is a missing probability, $1-Q$. For $z>1$, the full solution is

$$p_{\rm div}(\tau)=q_{h,\Lambda}(\tau)+[1-Q(h,\Lambda)]\delta(\tau-\tau_0), \tag{9}$$

and substitution into Eq. (3) yields $\Lambda(h)=\tau_0^{-1}\ln(hz)$ for the steady-state growth rate when $h>h_c$ [6].

Further analysis of Eq. (8) shows that a heritability threshold $h_c<1$ exists if and only if $\int_0^\infty d\tau k(\tau)/(\tau-\tau_0)$ converges [6], e.g., if $k(\tau)\sim(\tau-\tau_0)^\gamma$ near τ_0 for some $\gamma>0$. The steady-state population growth rate $\Lambda(h)$ qualitatively changes as h crosses the threshold: it depends on $k(\tau)$ for $h<h_c$ and becomes independent of it for $h>h_c$. The expected number of offspring having the same IDT as their parent is hz, and only parents with $\tau'=\tau_0$ can generate offspring with $\tau=\tau_0$. Thus, the fraction of the population with IDT τ_0 grows with rate $\tau_0^{-1}\ln(hz)$. If we add a small fraction of τ_0 cells to a population, they go extinct if $hz<1$, while if $hz>1$, they can constitute a giant cluster in the population's genealogy. The subpopulation localized at $\tau=\tau_0$ will be outcompeted by the rest of the population for $z^{-1}<h<h_c$, with $\Lambda(h)$ determined by Eq. (6), or it will dominate the population for $h>h_c$ and thus dictate its growth rate to be $\Lambda(h)=\tau_0^{-1}\ln(hz)$. In Fig. 1(a), we show a range of examples of $k(\tau)$ that admit a threshold h_c. Increasing h from 0 to 1, $\Lambda(h)$ increases monotonically with a shallow slope, while past h_c, the slope of the growth rate changes markedly.

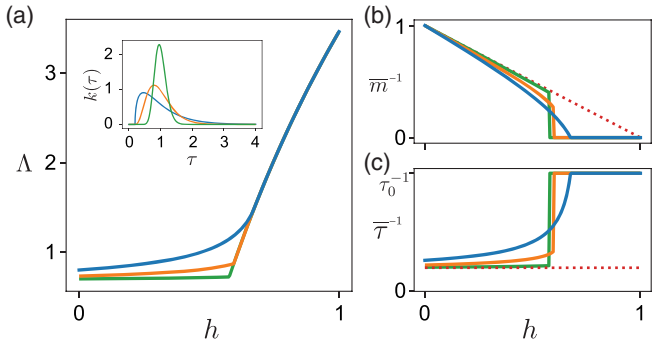

FIG. 1. Stationary solutions and their dependence on the heritability parameter h. Solid curves show results using $z=2$ for (a) population growth rate, $\Lambda(h)$; (b) reciprocal mean block size, $\bar{m}(h)^{-1}$; and (c) reciprocal lineage mean IDT, $\bar{\tau}(h)^{-1}$. Dotted line in (b),(c) indicates the result for isolated single cells (i.e., $z=1$). The IDT distribution $k(\tau)$ [shown at inset of (a)] is chosen to be a gamma distribution, shifted by $\tau_0=0.2$, with shape parameters $\alpha=1.5$ (blue), 4 (orange), and 20 (green); $k(\tau)=\Gamma(\alpha)^{-1}\theta^{-\alpha}(\tau-\tau_0)^{\alpha-1}e^{-(\tau-\tau_0)/\theta}$ for $\tau\ge\tau_0$. For the mean IDT to be 1, the scale parameter θ is chosen as $\tau_0+\alpha\theta=1$. $h_c=0.68$, 0.60, and 0.58, respectively, for $\alpha=1.5$, 4, and 20.

Localization phase transition of population age structure.—We now show that the threshold behavior identified above constitutes a phase transition in the strict sense. We map the population to a statistical mechanical ensemble as follows. From the viewpoint of single cell lineages, i.e., the history of an individual and all of its ancestors, an age-structured population is an ensemble of trajectories—the sequence of IDTs along a lineage $(\ldots,\tau_{i-1},\tau_i,\tau_{i+1},\ldots)$ is analogous to a microscopic state of a large system (e.g., a configuration of spins on a lattice or a conformation of a polymer in space)—while a single ancestral cell division τ_i specifies the state of a single component (e.g., a spin or a monomer) [6,37].

To analyze the structure of lineages observed above and below h_c, we consider the number of generations with which the same IDT is consecutively inherited, which we denote by m and call the "block size." The probability distribution of m over lineages, $p_{\rm lin}(m)$, is analogous to a correlation function, and its mean measures the typical correlation length. From Eq. (3), one can infer that the joint probability distribution of block size m and IDT τ is

$$p_{\rm lin}(m,\tau) \coloneqq (1-hze^{-\Lambda\tau})(hze^{-\Lambda\tau})^{m-1}p_{\rm div}(\tau). \tag{10}$$

For $h<h_c$, the mean block size $\bar{m}(h)$ is finite, while for $h>h_c$, $\bar{m}(h)$ diverges. The probability distribution of IDTs on lineages [6] is given by

$$p_{\rm lin}(\tau)=\begin{cases}\frac{(1-h)k(\tau)ze^{-\Lambda\tau}}{(1-hze^{-\tau\Lambda})^2\bar{m}}, & 0\le h<h_c\\ \delta(\tau-\tau_0), & h_c<h<1\end{cases}. \tag{11}$$

The expression indicates that the IDT distribution on lineages in the population is localized entirely at $\tau=\tau_0$

above h_c, despite the fact that the IDT distribution of isolated lineages remains $k(\tau)$.

The mean block size $\bar{m}(h)$ serves as an order parameter that diverges for $h > h_c$, and the continuity of the phase transition can be characterized by its behavior near h_c. If $\lim_{h\to h_c^-} \bar{m}(h) = \infty$, the transition is a continuous phase transition, while if $\lim_{h\to h_c^-} \bar{m}(h) < \infty$ the transition is referred to as discontinuous or "first order." Analogously, the lineage mean IDT, $\bar{\tau}(h)$, which is given by $\partial\Lambda/\partial \ln z$, exhibits the same type of phase transition. In terms of thermodynamics, the length of lineages t defines the system size, and $\ln z$ can be seen as a generalized force (e.g., a chemical potential). Then $t\Lambda$ is the thermodynamic potential (e.g., grand potential) whose first-order derivative by $\ln z$ coincides with the expected number of divisions on lineages averaged across the population, which is the extensive variable associated with $\ln z$ [6]. Examples of the h dependence of $\bar{m}(h)$ and $\bar{\tau}(h)$ are shown in Fig. 1(b),(c). Assuming the law of large numbers, $\bar{\tau}(h)^{-1} \simeq D/t$ and $\bar{m}(h)^{-1} \simeq S/D$ hold where D and S denote, respectively, the number of divisions and the number of switches to different values of τ on lineage [6].

Using the form of $k(\tau)$ given in Fig. 1, where $k(\tau) \sim (\tau - \tau_0)^\gamma$ for τ near τ_0, and computing $\bar{m}(h)$, we find that the phase transition is continuous for $0 < \gamma \leq 1$ and becomes discontinuous for $\gamma > 1$ [see Fig. 1(b)]. For a discontinuous transition, one expects to observe the coexistence of two phases at the transition point, which is seen in numerical simulations of finite populations shown below [Fig. 2(a)]. We can also compute the probability distribution of block sizes, which decays exponentially below the transition and follows power law statistics, $p_{\rm lin}(m) \sim m^{-\gamma-1}$ for large m, in the limit $h \to h_c^-$ as expected for correlation functions in the vicinity of a phase transition [6]. Such an

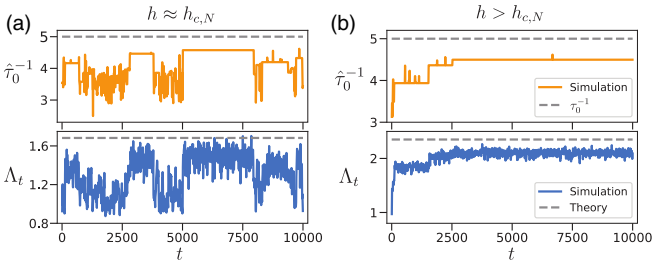

FIG. 2. Dynamics and aging of growth rates in a finite population. (a),(b) Time courses of reciprocal empirical minimal IDT, $\hat{\tau}_0^{-1}$ (top panels, orange, solid), compared to the minimal IDT, τ_0^{-1} (gray dashed line); and growth rates (bottom panels, blue line) compared to predicted stationary value (gray dashed line). (a) Coexistence of delocalized and localized states near the transition ($h = 0.7$); (b) aging dynamics above the transition ($h = 0.8$). Parameters are as in Fig. 1 using $\alpha = 4$, which exhibits a first-order localization transition. Population size in simulations is maintained at $N = 100$, and the effective heritability threshold is $h_{c,N} = 0.73$ (see [6] for simulation details).

appearance of long memory of IDT inheritance at the transition point is likewise observed in simulations [Fig. 2(a)].

Dynamics and aging of population growth rate.—In finite sized populations, the stationary distribution, Eq. (9), for $h > h_c$ is not achievable because any parent cell with IDT $\tau' > \tau_0$ has probability zero of generating offspring with IDT τ_0. Additionally, the distribution, Eq. (9), cannot be maintained as a steady state because cells with IDT τ_0 can be lost from the population within finite time due to coalescence. To observe dynamics in finite populations, we conducted exact stochastic simulations in which cells are randomly removed to maintain a fixed population size [6]. We sampled the initial population with size $N = 100$ independently from the stationary probability distribution with $h = 0$, which we refer to as the "delocalized state," and simulated the population forward in time for a given value of $h > 0$.

In simulations with $h < h_c$, growth rates Λ_t fluctuate around the expected steady-state growth rate (see [6]). Near the heritability threshold, however, Λ_t exhibits sudden transitions between two distinct, long-lived states [Fig. 2(a)], which is expected for systems near a first-order phase transition. One of these states represents localization at the empirical minimum IDT, denoted by $\hat{\tau}_0$, which is the minimum IDT among all the dividing cells within each time bin [6]. In this state, the growth rate fluctuates around $\hat{\tau}_0^{-1} \ln(hz)$ over a sufficient period during which $\hat{\tau}_0$ is constant. The other phase represents delocalization, where $\hat{\tau}_0$ exhibits large fluctuations. For higher values of h, the observed growth rate increases stepwise and fluctuates around $\hat{\tau}_0^{-1} \ln(hz)$ [Fig. 2(b)]. In this case, a fraction of the population localized at $\hat{\tau}_0$ is maintained over a significant time interval until a new value of $\hat{\tau}_0$ replaces the current empirical minimum IDT. The time intervals between these replacement events become increasingly long as $\hat{\tau}_0$ approaches τ_0 because IDTs that are shorter than the current minimum become increasingly rare. Plotting values of Λ_t at different simulation times as a function of h, the curve possesses an inflection point $h_{c,N}$ slightly greater than h_c, which we refer to as the effective transition point at fixed population size N (see [6] for further details).

Collective divisions, cell cycle synchronization, and noisy inheritance.—In addition to aging dynamics, above the transition divisions occur collectively and periodically in finite populations. The number of divisions that occur, binned in short intervals, is plotted over time (Fig. 3, left panels), along with its autocorrelation function (Fig. 3, right panels). The autocorrelation function does not oscillate below the transition but exhibits decaying oscillations near the transition point and sustained oscillations above the transition. The fact that the period of the autocorrelation function is approximately τ_0 reflects localization at $\hat{\tau}_0$ close to τ_0. We note that division rate oscillations have also been predicted to arise in cell-size control models due to negative IDT correlations [38].

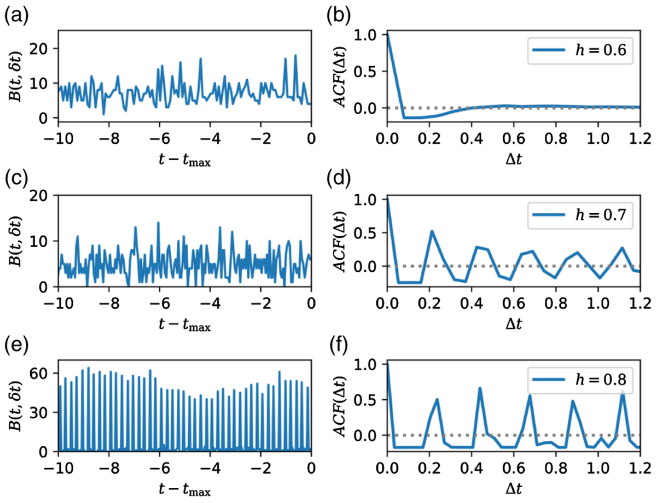

FIG. 3. Cell cycle synchronization in finite populations. Parameters are as in Fig. 2. Number of divisions $B(t, \delta t)$ binned over $\delta t = 0.1$ doubling time (a),(c),(e) and their autocorrelations (b), (d),(f) are shown. Simulations were run over $t_{\max} = 10^4$ time units, and the last 10 time units of the series are shown for (a), (c), and (e), where time point 0 indicates the simulation end. The autocorrelation function $ACF(\Delta t)$ was computed over the entire time series. The correlation coefficient was normalized to equal 1 at $\Delta t = 0$. Dotted line indicates zero correlation. (a),(b) Below the transition ($h = 0.6$), the timing of divisions is not synchronized. (c),(d) Near the transition point ($h = 0.7$), the timing of divisions is partially synchronized, observed as decaying oscillation of the autocorrelation function. (e),(f) Above the transition ($h > h_{c,N}$), collective divisions are observed, indicating the self-synchronization of cell cycles.

We tested the robustness of the transition properties to the inaccuracy of the inheritance of IDTs by allowing small fluctuations of the offspring's IDT when it inherits its parent's IDT with probability h. To do so, we modified the transition kernel to be

$$K(\tau, \tau') = h p_{\text{norm}}(\tau - \tau', \sigma) + (1 - h)k(\tau), \qquad (12)$$

where $p_{\text{norm}}(x, \sigma)$ is a normal distribution density function with standard deviation σ, truncated at τ_0. As a result, the population can reach equilibrium over a reasonable timescale, that is, the long-term behaviors between the two distinct initial conditions coincide [6]. Collective divisions are weaker but still detectable through the decaying oscillations of the autocorrelation function of divisions in the population. Additionally, we analyzed the behavior of a general Gaussian kernel, truncated at τ_0, with parameters specifying the mean, variance, and parent-offspring correlation of IDTs (the latter can be negative or positive). In all cases, for sufficiently high heritability, we found that as the population size increases from $N = 1$ to $N = 1000$, Λ exhibits a pronounced increase [see Fig. 4(a) and additional results in [6]]. In contrast, for low heritability or for negative IDT correlations, Λ varies little with N.

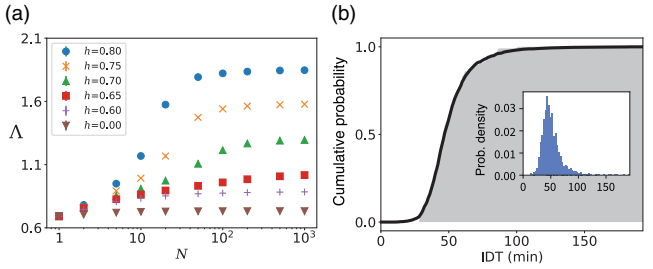

FIG. 4. (a) Dependence of Λ on population size N. Simulations use Eq. (12) with $\sigma = 0.1\tau_0$ and parameters as in Fig. 2. (b) Fitting the Lebowitz-Rubinow model using single-cell lineage data (F3 rpsL-gfp, glucose, 37°C from [3]). Empirical (shaded) and fitted (solid) cumulative distribution of $p_{\text{lin}}(\tau)$. Inset: empirical $p_{\text{div}}(\tau)$. Fitting yields $h = 0.23$; for comparison, the Pearson correlation of mother-daughter IDTs is 0.26. See [6] for methods and additional data.

Similar behavior is observed for $\bar{\tau}^{-1}$, indicating that even without exact inheritance of parental IDTs, signatures of the phase transition are observed when varying the population size [6].

Discussion.—In this Letter, we analyzed how the strength of IDT heritability affects age-structured population dynamics. In a model with heritable cell cycle durations first introduced in [34], we demonstrate the existence of a localization phase transition with a heritability threshold above which the population's distribution of IDTs localizes at the minimal IDT, corresponding to the fastest possible single-cell growth rate. We show that the lineage mean IDT provides an order parameter of the transition and above the heritability threshold predicts the emergence of single-cell lineages that maintain perfect inheritance of a minimal IDT.

A similar transition in exponentially growing populations is known in mutation-selection models of theoretical population genetics [7,39,40]. For example, Kingman's house-of-cards model [40], which describes population dynamics on a specific type of fitness landscape, exhibits localization at maximal fitness below a critical mutation rate. The results can be generalized to cases in which fitness is correlated between parent and offspring using the theory of positive linear operators [8].

The Lebowitz-Rubinow model is an idealization in which IDTs are either inherited precisely (with probability h) or not at all, and a key property of the model that underlies localization is the existence of a positive, minimal IDT, τ_0. In [6], using experimental measurements in *E. coli*, we show that by fitting empirical lineage IDT distributions [using Eqs. (4) and (11)], the model correctly infers h [see Fig. 4(b)]. Additionally, the data support the existence of $\tau_0 > 0$. Thus, the Lebowitz-Rubinow kernel captures key features of real biological data and correctly predicts its underlying parameters.

We showed that the signature of the localization transition can be experimentally observed by measuring the

population growth rate Λ at different population sizes in the range $N = 1$–1000, which is feasible in microfluidic experiments [3,41,42]. Varying the population size enables one to control the strength of selection in the experiments, as the size of heritable fitness differences that selection can act on efficiently scales with N^{-1}. Negative IDT correlations, as often observed in bacteria (Table S1 in [6]), correspond to a lack of heritability and do not yield transitionlike behavior for increasing N [6]. Above the IDT heritability threshold, population growth rates exhibit aging dynamics similar to evolutionary dynamics in a random, unbounded fitness landscape in the low mutation rate limit [43,44]. While aging dynamics occur for precise IDT heritability, transitionlike behavior is present in less accurate IDT inheritance systems typical of biological systems [6].

Remarkably, the Lebowitz-Rubinow model does not include cell-cell interactions, which are thought to be a major mechanism for cell cycle synchronization, yet our analysis predicts that strong but imperfect IDT heritability may be sufficient to cause self-synchronization of cell cycles in finite populations. This finding provides a starting point for the design of new types of synthetic biological oscillators that leverage population-level selective forces to establish robust cell cycle synchronization with sustained oscillations.

We thank A. Skanata and Y. Wakamoto for discussions. This work was supported by NIH R01-120231.

[1] S. Taheri-Araghi, S. Bradde, J. T. Sauls, N. S. Hill, P. A. Levin, J. Paulsson, M. Vergassola, and S. Jun, Curr. Biol. **25**, 385 (2015).
[2] L. Susman, M. Kohram, H. Vashistha, J. T. Nechleba, H. Salman, and N. Brenner, Proc. Natl. Acad. Sci. U.S.A. **115**, E5679 (2018).
[3] M. Hashimoto, T. Nozoe, H. Nakaoka, R. Okura, S. Akiyoshi, K. Kaneko, E. Kussell, and Y. Wakamoto, Proc. Natl. Acad. Sci. U.S.A. **113**, 3251 (2016).
[4] A. Amir, Phys. Rev. Lett. **112**, 208102 (2014).
[5] J. Grilli, C. Cadart, G. Micali, M. Osella, and M. C. Lagomarsino, Front. Microbiol. **9**, 1541 (2018).
[6] See Supplemental Material, which includes Refs. [3,7–31], at http://link.aps.org/supplemental/10.1103/PhysRevLett.125.268103 for supplemental text, figures and tables.
[7] J. Hermisson, O. Redner, H. Wagner, and E. Baake, Theor. Popul. Biol. **62**, 9 (2002).
[8] R. Bürger and I. M. Bomze, Adv. Appl. Probab. **28**, 227 (1996).
[9] T. Nozoe, E. Kussell, and Y. Wakamoto, PLoS Genet. **13**, e1006653 (2017).
[10] P. K. Mogensen and A. N. Riseth, J. Open Source Software **3**, 615 (2018).
[11] A. Seita, H. Nakaoka, R. Okura, and Y. Wakamoto, bioRxiv, https://doi.org/10.1101/2020.07.10.196881 (2020).
[12] N. Mosheiff, B. M. C. Martins, S. Pearl-Mizrahi, A. Grünberger, S. Helfrich, I. Mihalcescu, D. Kohlheyer, J. C. W. Locke, L. Glass, and N. Q. Balaban, Phys. Rev. X **8**, 021035 (2018).
[13] H. E. Kubitschek, Exp. Cell Res. **26**, 439 (1962).
[14] F. B. Yu, L. Willis, R. M. W. Chau, A. Zambon, M. Horowitz, D. Bhaya, K. C. Huang, and S. R. Quake, BMC Biol. **15**, 11 (2017).
[15] E. D. Hawkins, J. F. Markham, L. P. McGuinness, and P. D. Hodgkin, Proc. Natl. Acad. Sci. U.S.A. **106**, 13457 (2009).
[16] H. Sasaki, H. Yoshinaga, and K. Kawano, Radiat. Res. **72**, 364 (1977).
[17] R. G. Staudte, M. Guiguet, and M. C. D'Hooghe, J. Theor. Biol. **109**, 127 (1984).
[18] M. Hola and P. A. Riley, J. Cell Sci. **88**, 73 (1987), https://jcs.biologists.org/content/88/1/73.long.
[19] S. Chakrabarti, A. L. Paek, J. Reyes, K. A. Lasick, G. Lahav, and F. Michor, Nat. Commun. **9**, 5372 (2018).
[20] G. Froese, Exp. Cell Res. **35**, 415 (1964).
[21] R. Van Wijk and K. W. Van De Poll, Cell Proliferation **12**, 659 (1979).
[22] M. Absher, D. Sylwester, and B. A. Hart, Environ. Res. **30**, 34 (1983).
[23] M. Absher and V. J. Cristofalo, J. Cell. Physiol. **119**, 315 (1984).
[24] O. Sandler, S. P. Mizrahi, N. Weiss, O. Agam, I. Simon, and N. Q. Balaban, Nature (London) **519**, 468 (2015).
[25] H. Miyamoto, E. Zeuthen, and L. Rasmussen, J. Cell Sci. **13**, 879 (1973), https://jcs.biologists.org/content/13/3/879.long.
[26] A. van Meeteren, R. van Wijk, J. Stap, and B. F. Deys, Cell Proliferation **17**, 105 (1984).
[27] J. Grasman, Bull. Math. Biol. **52**, 535 (1990).
[28] R. Shields and J. A. Smith, J. Cell. Physiol. **91**, 345 (1977).
[29] R. G. Staudte, R. M. Huggins, J. Zhang, D. E. Axelrod, and M. Kimmel, Math. Biosci. **143**, 103 (1997).
[30] R. Sennerstam and J. O. Strömberg, J. Theor. Biol. **131**, 151 (1988).
[31] K. B. Dawson, H. Madoc-Jones, and E. O. Field, Exp. Cell Res. **38**, 75 (1965).
[32] B. Charlesworth, *Evolution in Age-Structured Populations*, 2nd ed., Cambridge Studies in Mathematical Biology (Cambridge University Press, Cambridge, England, 1994).
[33] M. Eigen, J. McCaskill, and P. Schuster, Adv. Chem. Phys. **75**, 149 (1989).
[34] J. L. Lebowitz and S. I. Rubinow, J. Math. Biol. **1**, 17 (1974).
[35] IDTs of sibling cells may be correlated, which does not change Eq. (2), as long as the number of offspring is independent of the parent's IDT.
[36] R. Fisher, *The Genetical Theory of Natural Selection* (Clarendon, Oxford, 1930).
[37] Y. Wakamoto, A. Y. Grosberg, and E. Kussell, Evolution **66**, 115 (2012).
[38] F. Jafarpour, Phys. Rev. Lett. **122**, 118101 (2019).
[39] M. Eigen, Naturwissenschaften **58**, 465 (1971).
[40] J. F. C. Kingman, J. Appl. Probab. **15**, 1 (1978).
[41] M. Wallden and J. Elf, Curr. Opin. Biotechnol. **22**, 81 (2011).
[42] G. Lambert and E. Kussell, PLoS Genet. **10**, e1004556 (2014).
[43] S. C. Park and J. Krug, J. Stat. Mech. 04 (2008) P04014.
[44] T. Brotto, G. Bunin, and J. Kurchan, J. Stat. Mech. 03 (2016) 033302.